

EUCALL

The European Cluster of Advanced Laser Light Sources

Grant Agreement number: 654220

Work package 7 – PUGCA

Deliverable D7.9

Test of XGM prototype at different light sources

Lead Beneficiary: DESY

Authors:

Stephan Klumpp, Andrey Sorokin, Kai Tiedtke (DESY)

M. Richter (PTB)

Takahiro Tanaka (AIST / NMIJ / PTB)

Due date: 30th September, 2018

Date of delivery: 18th September 2018

Project webpage: www.eucall.eu

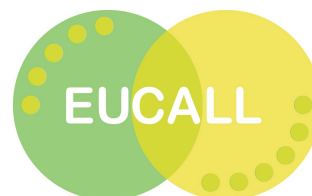
<i>Deliverable Type</i>	
R = Report DEM = Demonstrator, pilot, prototype, plan designs DEC = Websites, patents filing, press & media actions, videos, etc. OTHER = Software, technical diagram, etc.	R
<i>Dissemination Level</i>	
PU = Public, fully open, e.g. web CO = Confidential, restricted under conditions set out in Model Grant Agreement CI = Classified, information as referred to in Commission Decision 2001/844/EC	PU



LUND UNIVERSITY



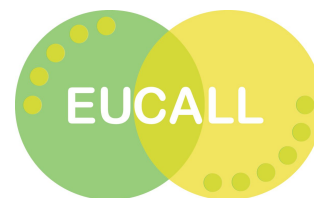
This project has received funding from the *European Union's Horizon 2020 research and innovation programme* under grant agreement No 654220



Contents

1	Introduction	3
2	Objectives	4
3	Prototype Tests at different light sources	5
3.1	Detector calibration	5
3.2	Detector performance at European XFEL	7
3.2.1	Beamline layout of the Femtosecond X-ray Experiment (FXE)	8
3.2.2	Transmission performance of the FXE beamline	10
3.2.3	Correlation between Gas Monitor Detector (XGM) and room temperature Radiometer on absolute scale	11
3.2.4	Pulse resolved measurements	12
3.3	Detector performance at BL1 of SACLA	14
4	Synergy Aspects	15
5	Conclusions	17
6	Summary	18





1 Introduction

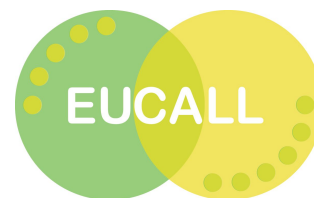
Determining the properties of x-ray beams is the key set of information research infrastructures for x-rays have to provide to their users to enable them to interpret their data. Depending on the mechanism to produce x-rays (for a short summary see e.g. [1]), the properties span a large dynamic range which is hard to measure with just one single method per information value. The scope of the Pulse Characterisation and Control (PUCCA) workpackage of the European Cluster of Advanced Laser Light Sources (EUCALL) was to provide schemes and prototypes to characterise

- the wavefront of an x-ray beam,
- the intensity of an x-ray beam,
- and the timing jitter of the delay between an x-ray pulse and a second pulse from an independent source, like a short pulse laser,

suitable to be used at synchrotron storage rings, free-electron laser and optical laser based facilities.

Special interest of EUCALL was to bring together experts of the various fields named above to find synergies between the different methods of producing and characterising x-rays to develop improved diagnostics methods in an open-source framework.





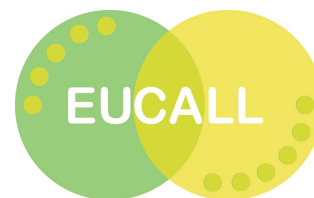
2 Objectives

Two main objectives have been formulated for PUGCA regarding the intensity measurement of x-ray beams. On the one hand, new advanced schemes to detect short x-ray pulses on a shot-to-shot basis on absolute scale with a high repetition rate up to 5 MHz (Task 7.3.1). And, on the other hand, as next a step, to build a prototype to test these schemes (Task 7.3.2). Expertise for such a device is placed at DESY where the Gas Monitor Detector (GMD) [2] is the working horse to determine the intensity of the short x-ray pulses (in the order of 100 fs) of FLASH in the soft x-ray regime (24 eV to 295 eV) with high repetition rate between 100 kHz up to 1 MHz. Depending on the photon energy, on average 1 μ J to 200 μ J of x-ray pulse intensity is delivered to the users.

Compared to the soft x-ray free electron laser FLASH, the different research infrastructure facilities have different parameters and demands. While synchrotron storage rings have time structure in the ps domain and photon flux in the order of 1×10^{12} photons/s to 1×10^{14} photons/s, not per pulse, their photon energy range spans a larger dynamic range from soft to hard x-rays. Hard x-ray free electron laser facilities, like European XFEL, LCLS, SACLA, or SwissFEL, have bunch train time structures, high intensity per pulse, and high repetition rates of the pulses (60 Hz to 100 Hz at LCLS and SACLA, 4.5 MHz at European XFEL), but operate at photon energies where the cross section of the usual used target gas xenon drops by several orders of magnitude. Laser driven x-ray sources can be operated with high repetition rate in the soft and hard x-ray regime with pulse length in the order of fs, but, compared to FELs, their intensity per pulse is rather low in the order of 1×10^4 to 1×10^6 photons per pulse (for a short summary see e.g. [1]).

Between all these operations parameters a compromise has to be found for one device or several specialised devices have to be developed.





3 Prototype Tests at different light sources

Following the scope of our PUCCA deliverable D7.1 [1], the presented detector schemes were proposed to the PUCCA community during our FXE commissioning meeting, November 2016, in Hamburg. Upon discussing the best suited scheme for the Femtosecond X-Ray Experiment (FXE) commissioning for summer and autumn 2017, the decision of the meeting was to use an GMD [2] including a commercial multiplier as proof-of-principle prototype [1, 3].

To measure the intensity of the x-ray photon beam of European XFEL, the intensity monitor was calibrated at a known photon source, the Metrology Light Source (MLS) of the Physikalisch Technische Bundesanstalt (PTB), Berlin, and then used to determine the transmission of the photon beamline of the FXE of European XFEL.

In addition, the performance of the XGM has been tested at the soft x-ray beamline BL1 of the SPring-8 Angstrom Compact free-electron LASer (SACLA), Japan.

3.1 Detector calibration

As discussed in deliverable D7.1 [1], the basic physical mechanism to determine the intensity of a photon beam using a gas-phase detector [2, 4] is photoionisation:

$$N_{ion} = N_{ph} \cdot n \cdot \sigma(\hbar\omega) \cdot l \quad (3.1)$$

- N_{ion} : number of detected ions
- N_{ph} : number of incident photons of energy $\hbar\omega$
- n : density of the gas phase target in the interaction volume
- $\sigma(\hbar\omega)$: total photoionisation cross section of the gas phase target
- l : effective absorption length of the interaction volume along the photon beam axis accepted by ion detector

In order to be able to determine the number of incident photons N_{ph} , and hence the intensity of the photon beam on absolute scale, by detecting the photoionised ion current

$$I_{ion} = N_{ion} \cdot e \cdot \gamma \quad (3.2)$$

- I_{ion} : detected averaged ion current
- e : elementary charge $e=1.602\,176\,620\,8 \times 10^{-19}$ C [5]
- γ : ion mean charge



all parameters of equation (3.1) and equation (3.2) have to be determined.

The parameters can be divided into two different groups. On the one hand, the physical properties of the used target (gas) as the photoionisation cross section $\sigma(\hbar\omega)$ and the averaged generated charge γ per incident photon $\hbar\omega$. And on the other hand, the experimental parameters of the used set-up like the target density

$$n = \frac{N_t}{V} = \frac{p}{k_B T} \quad (3.3)$$

N_t : number of the target particles

V : chamber volume (not need)

p : target pressure

k_B : Boltzmann constant $k_B = 1.380\,648\,52 \times 10^{-23} \text{ J K}^{-1}$ [5]

T : temperature of the target

and the effective absorption length l .

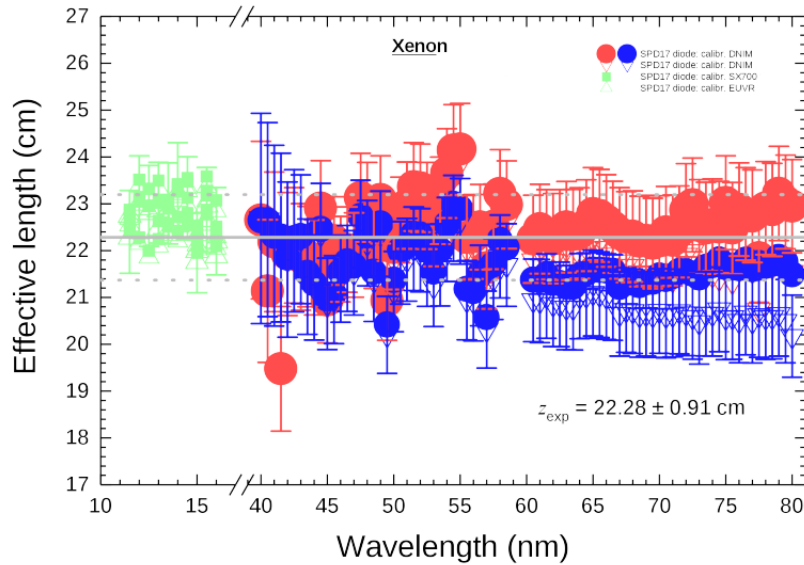
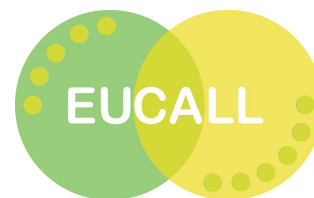


Figure 3.1: Effective absorption length of the XGM determined at the Metrology Light Source (MLS) of the PTB, Berlin. The incident photon flux was measured with different types of photodiodes on absolute scale (red, blue dots, green triangles and squares). The effective absorption length was evaluated to be $l = (22.28 \pm 0.91) \text{ cm}$.

While the physical parameters can be considered to be known from literature [2] (and references therein), the thermodynamical state functions p and T of the target gas have to be measured together with the particle current I_{ion} . Hence, the effective absorption length l is the only remaining parameter which has to be determined in a calibration procedure. To achieve this, again, equation (3.1) and equation (3.2) are used, but for the calibration, now, the number of



incident photons N_{ph} has to be known. For up to the soft x-ray regime of the electromagnetic spectrum the Physikalisch Technische Bundesanstalt (PTB), Berlin, provides at the Metrology Light Source (MLS) x-ray beams of known intensities. Figure 3.1 shows the effective absorption length l measured for different photon energies $\hbar\omega$. On average the effective absorption length can be given with $l = (22.28 \pm 0.91)$ cm.

3.2 Detector performance at European XFEL

The X-Ray Gas Monitor Detector (XGM) prototype was designed to be able to determine the pulse resolved intensity of a hard x-ray sources with a high repetition rate in the MHz-range [1, 6]. To test the performance of the XGM prototype at these conditions, it was set up at the end of the beamline of the Femtosecond X-Ray Experiment (FXE) [7] of European XFEL (see figure 3.2). Behind the XGM the room temperature radiometer of the National Institute of Advanced Industrial Science and Technology (AIST) [8–10] was in addition set up to verify and control the averaged determined pulse intensity.

The XGM chamber was mounted on one of the optical tables of FXE at the end of the experimental hutch. At the XGM entrance CF40 flange an approximately 3 m long tube was installed which was filled homogeneously together with the XGM main chamber with xenon gas. This improved the transmission of the hard x-rays from the sample stage of FXE into the XGM (see figure 3.4 and table 3.1). Only a small, approximately 2.4 m long, section of air was left free to be able to place the Large Pixel Detector (LPD) into the beam path, if desired by the experiment performed at the sample stage. At the XGM exit CF40 flange a cross with a move-able holder with calibrated photodiodes, provided by the Physikalisch Technische Bundesanstalt Berlin (PTB), was mounted and behind them, as photon dump, the room temperature radiometer (see figure 3.2).

In one of the side flanges of the XGM prototype chamber, the test multiplier set-up was placed. As pointed out in our deliverable D7.1 [1], the multiplier enhances the capability of the XGM at low count rates which occur either at high photon energies in the hard x-ray regime, because of the low photoionisation cross section, or at light sources with intrinsic low photon flux. The multiplier concept was tested at FXE and reported in our deliverable D7.4 [3].

The xenon gas pressure was regulated by an automatic needle valve (*Pfeiffer RVC300*) and controlled by a calibrated spinning rotor gauge (SRG) from *MKS instruments*. The photoionised Xe ion current was read out by *Keithley 1740A* picoamperemeters. The fast electron signal was recorded with a 4 GHz-oscilloscope from *Teledyne LeCroy*. The base pressure of the XGM chamber without the xenon as was in the order of 2×10^{-6} hPa. The xenon pressure during operation of the XGM was in the range of 5×10^{-3} hPa to 2×10^{-2} hPa.



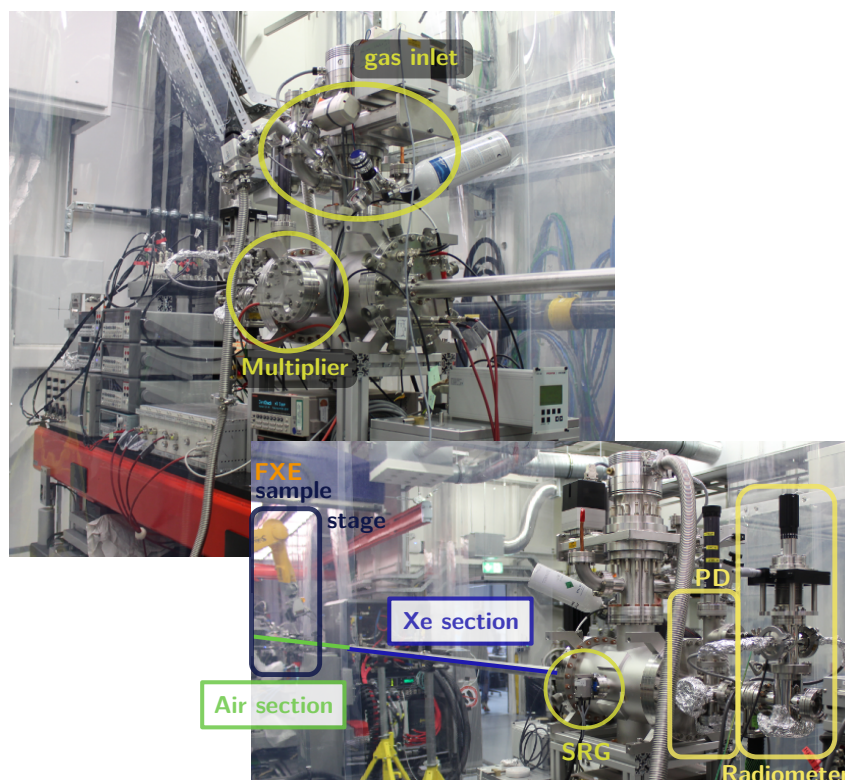


Figure 3.2: Set-up of the XGM prototype at the Femtosecond X-Ray Experiment (FXE) of European XFEL at the end of the experimental hutch. From the FXE sample stage to the XGM the photons from the SASE1 undulator (see figure 3.3) have to pass an air section to be able to place the Large Pixel Detector (LPD) into the beam path and a xenon section in front of the XGM (details see main text). Behind the XGM a set of calibrated photodiodes (PD) [11] provided by the Physikalisch Technische Bundesanstalt (PTB), Berlin, and a radiometer [8–10] from AIST as primary standard and photon dump was installed.

3.2.1 Beamline layout of the Femtosecond X-ray Experiment (FXE)

The beamline layout of the SASE1 undulator, for short, hard x-ray pulses, and the Femtosecond X-Ray Experiment (FXE) of European XFEL is described in [7] and depicted in the figures 3.3 and 3.4. The main operating parameters of the accelerator to produce the x-ray pulses during the commissioning of FXE have been:

photon wavelength	1.34 Å
photon energy	≈9.25 keV
bunch pattern	30 per train 120 per train (20.11.2017, only)
bunch separation	1.1 MHz / ≈ 0.91 μs

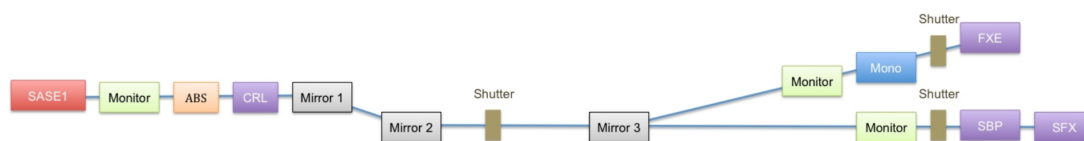
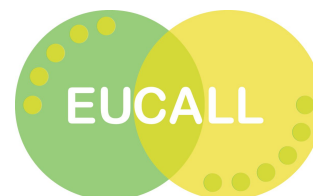


Figure 3.3: Sketch of the beamline layout of the FXE experiment [7]. The shown components are (from left to right): SASE1: SASE1 undulator. Monitor: gas-phase based XGM determining the intensity of the photon beam on absolute scale. ABS: solid-state absorber to attenuate the photon beam. CRL: compound refractive lenses. Mirror1: first deflecting mirror (M1). Mirror2: second deflecting mirror (M2). Shutter: first beam shutter to block the photon beam. Mirror3: switching mirror (M3) to select the experiment at SASE1 between SPB and FXE. Monitor: solid-state beam monitor. Mono: crystal monochromator. Shutter: first beam shutter to block the photon beam. FXE: FXE experimental hutch including local x-ray optics (see figure 3.4).

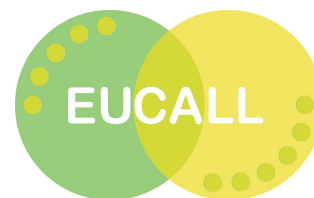


Figure 3.4: Sketch of the beamline layout of the FXE experimental hutch [7]. SASE1: undulator tunnel (see figure 3.3). The components in the FXE experimental hutch are (from left to right): SAA: solid attenuator assembly. BLS: Be lens system. DW: diamond windows as separation between the accelerator vacuum and the experimental area in air or helium atmosphere. He: helium section to sample stage. ST: sample stage. LPD: large pixel detector with beam path in air. XGM: prototype gas monitor detector with beam path in Xe atmosphere. PD: stage with calibrated photo diodes from PTB [11]. BM: room temperature radiometer from AIST as primary standard [8–10].

The intensity and the pointing of the photon beam are determined after the undulator by the permanent installed x-ray gas monitor detector of the photon beamline (monitor in figure 3.3). The x-ray beam can be attenuated by solid state metal foils (ABS in figure 3.3) and focused by compound refractive lens stacks (CRL in figure 3.3). To guide the photon beam towards the FXE experimental hutch two off-set mirrors (M1 and M2 in figure 3.3) and one switching mirror (M3 in figure 3.3) are used. Between M2 and M3 a shutter is placed to shut of the x-ray beam, if necessary. After the mirror M3 another solid-state beam monitor is placed and a monochromator to be able to disperse the the photon beam further but which was not used during the commissioning. All the named components are placed within the tunnel structure of European XFEL. The photons then enter the experimental hutch through the user valve (last shutter in figure 3.3).

The main optical elements in the FXE experimental hutch are a unit of solid-state attenuators (SAA in figure 3.4) and a unit of beryllium lenses (BLS in figure 3.4). As separation between the





vacuum of the beamline and the air atmosphere of the experimental hutch a diamond window (50 μm thick, 0.94133 transmission [12]), is placed at the end of the beamline. At a distance of approximately 2 m the sample stage (ST) of FXE follows behind which the Large Pixel Detector (LPD) can be placed. At the end of the experimental hutch the XGM, together with the PD and the room temperature radiometer was mounted as described above.

3.2.2 Transmission performance of the FXE beamline

Before the intensity of each short x-ray pulse can be determined the averaged beam intensity at the end of the experimental hutch has to be measured. Each optical element between the SASE1 undulator and the XGM will diminish the number of photons of each pulse. The absorption of the components can be estimated and by comparing the intensity right behind the undulator with the averaged beam intensity at the end of the hutch measured by the XGM and the radiometer, the overall performance of the beamline can be optimised.

Table 3.1 summarises the expected values for the transmission of the different beamline components. The values are determined by the geometry of the components and the material they are made of [12]. Most of them are designed to disturb the beam as little as possible, like the mirrors and the windows separating the vacuum from higher atmospheric pressures. Some components, for example the lenses, have in principle a high transmission, but because they have a smaller aperture than the beam size at their position in the beamline, they cut the beam (0.25 estimated transmission). Up to the sample stage (ST) of FXE, the lenses in the undulator tunnel are the only noteworthy components where the photon flux is diminished.

For the determination of the average value of the beam intensity with the XGM and the radiometer at the end of the experimental hutch of FXE, the free air section of approximately 2.4 m length is another area where many photons are lost, 0.18 transmission [12], even at hard x-ray energies of 9.25 keV. Multiplying all values of table 3.1, the XGM and the radiometer at the end of the FXE experimental hutch can only detect $\approx 3.5\%$ of the produced x-ray intensity, if all components are properly aligned.



beamline component (fig. 3.3/3.4)	transmission	Source
ABS	1	not used
CRLs	1	FXE / European XFEL
mirror M1	0.95	European XFEL
mirror M2	0.95	European XFEL
mirror M3	0.95	European XFEL
monochromator	1	not in beam path
SAA	1	not used
BLS	0.25	European XFEL
Diamond window (DM), 50 μm	0.941 33	[12]
He section, 2 m	0.99	[12]
ST	1	
air section, 2.4 m	0.180 93	[12]
Kapton window XGM, 75 μm	0.965	[12]
Xe section XGM, 3 m, 5×10^{-5} hPa	0.998 88	[12]
total estimated transmission	0.035	

Table 3.1: Estimated transmission of each optical element of the FXE beamline and commissioning experiment at a photon energy of 9.25 keV.

3.2.3 Correlation between Gas Monitor Detector (XGM) and room temperature Radiometer on absolute scale

Before the optimisation of the beamline set-up and the photon transmission from the SASE1 undulator to sample stage and to the intensity monitors at the end of the FXE experimental hutch, the correlation between the room temperature radiometer [8–10], as primary standard, and the XGM chamber [1, 2, 6, 13] was checked. Within the uncertainties of the methods applied to determine the photon flux on absolute scale the readings of the radiometer and the XGM correlate with each other (figure 3.5a). Only, at higher averaged pulse intensities the correlation of the data deviates from a perfect bisecting line (figure 3.5b).

The transmission of the FXE beamline was tested and optimised at different shifts. Table 3.2 summarises the results of the beamline optimisation.

The determined average transmission of the optical elements of the FXE beamline of 3.2 % agrees well with the estimated value of 3.5 % (table 3.1).

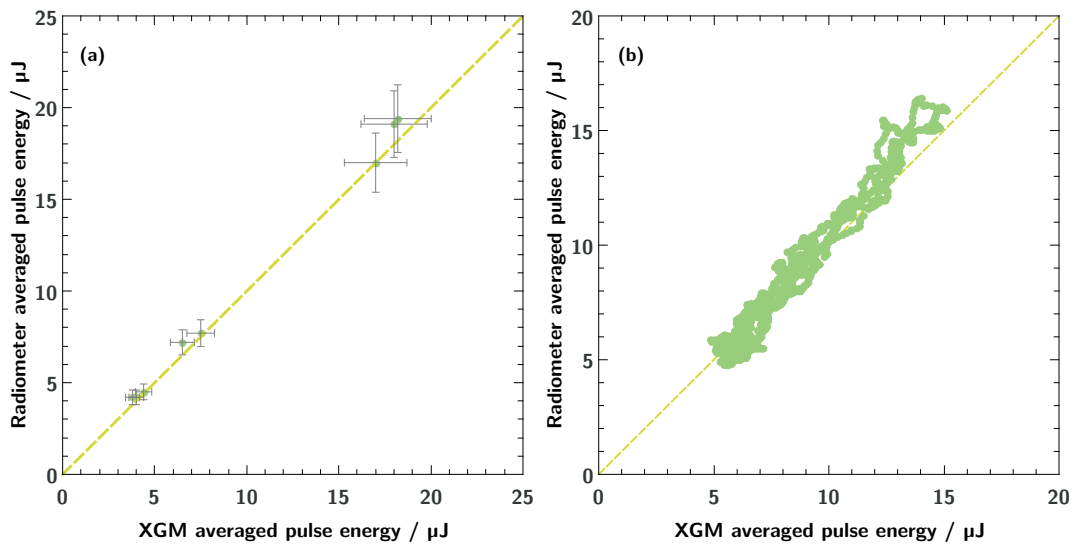


Figure 3.5: (a) Calibration / corelation of the XGM with the radiometer primary standard.
 (b) Correlation between the radiometer and the XGM for a period of 20 min.

date	monitor	photon pulse intensity / μJ		transmission
		XGM	radiometer	
16.11.2017	700	35	25	0.05
17.11.2017	670	17	17	0.025
20.11.2017	1140	22.2	26.7	0.02

Table 3.2: Results of the transmission optimisation of the optical elements of the FXE beamline.

3.2.4 Pulse resolved measurements

Within the XGM the photoelectrons and ions are separated by high electric fields [1, 2] and detected by Faraday-Cups. The slow ion side is used to determine the averaged absolute intensity of the incident photon beam (see [1]), whereas the fast electron side can be used to resolve the individual pulses of a high repetition bunch train as delivered by FLASH or European XFEL. The individual, relative pulse intensity of each electron pulse can then be calibrated on absolute scale by the calibrated integral slow ion signal, because both detected values are within the uncertainty of the measurement due to the same amount of photo induced charge.

Figure 3.6a shows the raw image of an oscilloscope trace of the electron Faraday-Cup of the XGM. The individual pulses of the European XFEL are visible as negative spikes. During our measurements, a bunch train of 120 bunches with 1 MHz (see inlay upper right corner of figure 3.6a) repetition rate was produced by European XFEL. The area of each peak in the electron trace is proportional to the pulse energy of the x-ray pulses. The integral ion current of the in-

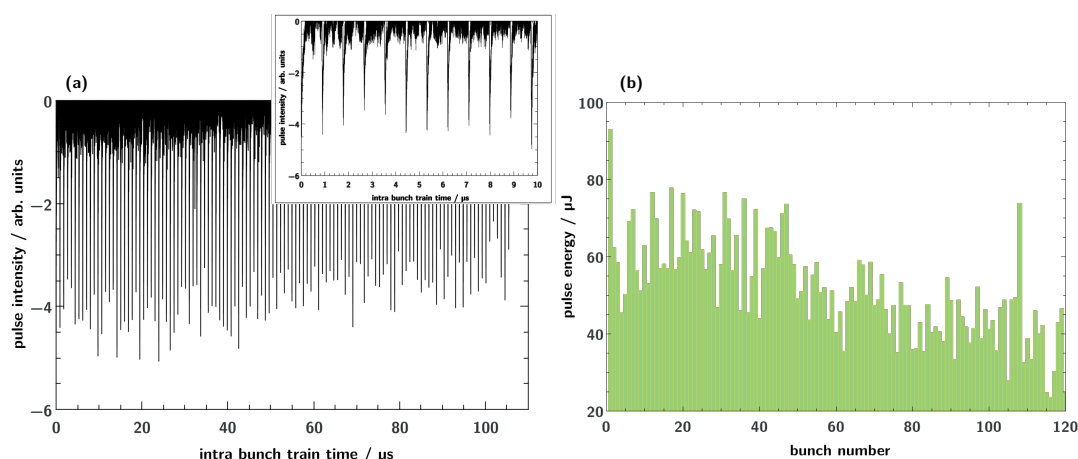


Figure 3.6: (a) Oscilloscope trace of the electron Faraday-Cup of the XGM. The individual pulses of the bunch train of European XFEL are visible as spikes in the negative direction. The pulses were generated with 1 MHz repetition rate by European XFEL. The upper right inlay is the magnification of the first 10 μs after the bunch train trigger. (b) Bunch pattern with pulse intensities on absolute scale as measured by the XGM at the end of the FXE hutch. The shown pattern gives the integral pulse intensities for the measured trace in (a).

Individual bunch train gives the normalisation factor to calibrate the electron trace to absolute values. The individual pulse energy is then found by summing up the area of the electron peak (figure 3.6b).

Because of the air atmosphere between the sample stage (ST) and the XGM at the end of the FXE hutch (including the xenon path of the XGM set-up as well), the transmission of photons from the ST to the XGM is $\approx 18\%$, only. Hence, the number of photons at the sample is approximately a factor of 5 higher than as determined by the XGM. The air section was needed to operate the LPD in parallel. With a bunch pattern delivered to the sample as depicted in figure 3.6b, the average number of photons at the sample is in the order of 3.5×10^{10} photons/pulse.

3.3 Detector performance at BL1 of SACLA

In April 2018, similar measurements as at FXE have been performed cross calibrating the XGM again with the room temperature radiometer [8–10] at the soft x-ray beamline (BL1) of the SPring-8 Angstrom Compact free-electron LASer (SACLA). In addition to the measurements at the FXE instrument of European XFEL (see section 3.2.3), the intensity of the FEL beam was measured at different photon energies in the soft x-ray regime. As can be seen in figure 3.7,

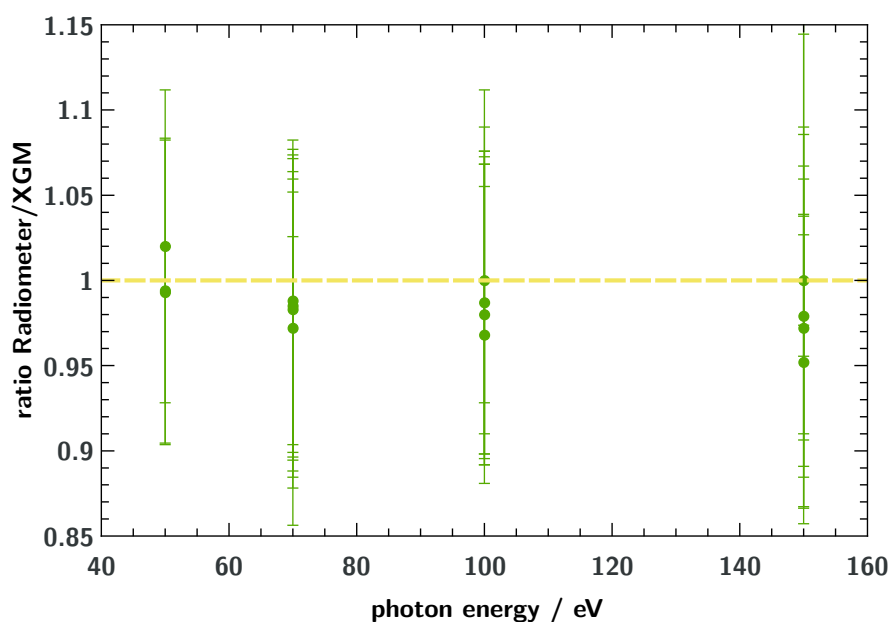


Figure 3.7: Ratio of the photon beam intensity of the soft x-ray beamline BL1 of SACLA measured with the XGM and a room temperature radiometer [8–10]. All ratios, independent of the photon energy, are almost 1 hence in very good agreement.

almost independent of the photon energy, the depicted ratios are 1 within the combined uncertainty limit of the intensity detector types. The room temperature radiometer is a primary standard to measure beam intensities hence the ratio proves the quality of the XGM detector calibration procedure.

4 Synergy Aspects

As demonstrated, the chosen intensity monitor design works well for synchrotron storage rings (MLS), hard x-ray FEL facilities like European XFEL or at the soft x-ray beamline of SACLA. At the free electron laser FLASH this device works well since a decade [14].

At laser driven x-ray sources, like ELI, the device will help to commission the HHG source in the E1 laboratory of ELI-Beamlines (Czech Republic), but for many laser table applications it will be too bulky to fit in. During the several EUCALL meetings, the idea of a miniaturised version of the intensity monitor was discussed which, in a first design study, might fit into a common CF63 double cross vacuum chamber (figure 4.1).

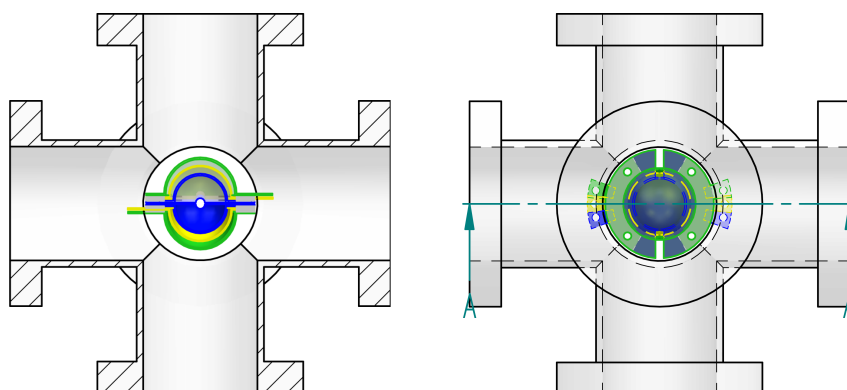
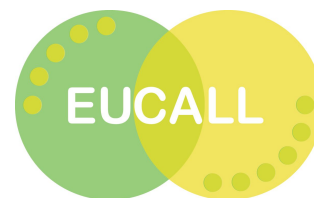


Figure 4.1: Conceptual design of a miniaturised transparent intensity monitor for tabletop laser applications.

The basic concept follows the discussion of deliverable D7.1 [1]. Because of the low photon flux per pulse of a table-top laser, compared to an FEL, and of the rather short effective absorption length of a miniaturised detector, the count rate will be rather low. Hence, it has to be amplified. As reported in deliverable D7.4 [3], the multiplier scheme works well.

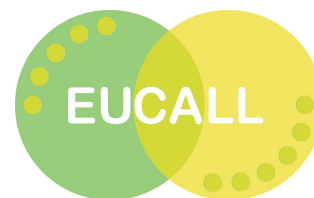
The key feature of the miniaturised detector design will be round dynodes and detection electrodes. Following equation (3.1), to optimise the ion yield per incident photon, the target pressure and the effective absorption length can be increased (maximised). Ambient gas pressures do not cope well with usually needed vacuum environments and introducing a multiplier scheme for particle amplification, at too high gas pressure, electric discharges can occur. Hence, an optimum between the gas pressure and a rather low voltage between the dynodes



has to be found. At low multiplier voltage, on the other hand, it can be expected, the photoionised electrons will fly into the full room angle which makes it necessary to cover a 4π geometry. These are demanding constraints for future dynodes and the material they will consist of.

This concept will be a well suited project for joint endeavours beyond EUCALL and is foreseen to be pursued by ELI-Beamlines and DESY.



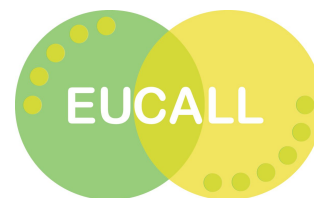


5 Conclusions

As concluded during the FXE commissioning meeting of PUCCA in Hamburg during November 2016, the chosen detector concept based upon the FLASH XGM worked at the FXE experiment of European XFEL (section 3.2) and BL1 of SACLA (section 3.3). The detector was successfully calibrated to determine pulse intensities on absolute scale at the MLS, Berlin (section 3.1). This calibration was verified and confirmed using different primary standards to detect beam intensities on absolute scale at European XFEL (figure 3.5) and SACLA (figure 3.7).

With the XGM mounted on the last optical table of the FXE instrument (figure 3.2) the intensity behind the interaction zone of FXE was measured and the total transmission of the FXE beamline was determined to be in the order of 3.5 % (table 3.1) at 9.25 keV. At hard x-ray photon energies from 9 keV to 12 keV the photoionisation cross section ranges in the same order of magnitude of 3×10^{-2} Mb [12], hence the XGM can be operated in this hard x-ray energy range.





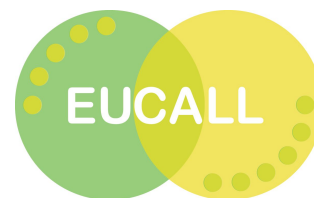
6 Summary

The main goal regarding intensity measurements of x-ray beams on absolute scale within the PUGCA workpackage of EUCALL was to develop new detector schemes suited for all research infrastructures, like synchrotron storage ring, FELs, and laser based sources, and to build and test prototype devices of these schemes.

Based on the FLASH XGMD design, a multiplier scheme was discussed [1] suited for hard x-ray FELs, like European XFEL, and integrated within a prototype used for commissioning of the FXE experiment of European XFEL. As reported in section 3.2 and [3], the new concept works promisingly.

On the other hand, the current design is still too large to fit into common laser tabletop applications hence a miniaturised concept has been discussed during the EUCALL meetings (figure 4.1). For this concept, a further prototype has to be built which is foreseen to be a future collaboration between ELI-Beamlines and DESY beyond the end of the EUCALL project.





Bibliography

- [1] S. Klumpp et al., *Ultimate XGM sensitivities at FEL and ELI sources*, (EUCALL Deliverable D7.1, 2016).
- [2] K. Tiedtke et al., *Journal of Applied Physics* **103**, 094511, 094511 (2008)
DOI: [10.1063/1.2913328](https://doi.org/10.1063/1.2913328).
- [3] S. Klumpp et al., *XGM prototype: calibrated and tested*, (EUCALL Deliverable D7.4, 2018).
- [4] A. A. Sorokin et al., *AIP Conference Proceedings* **705**, 557–560 (2004)
DOI: <http://dx.doi.org/10.1063/1.1757857>.
- [5] P. J. Mohr et al., *Rev. Mod. Phys.* **88**, 035009 (2016)
DOI: [10.1103/RevModPhys.88.035009](https://doi.org/10.1103/RevModPhys.88.035009).
- [6] S. Klumpp et al., *Construction of prototype XGM finished*, tech. rep. (EUCALL Milestone M7.2, 2017).
- [7] C. Bressler et al., *European X-Ray Free-Electron Laser Facility GmbH* (2012)
DOI: [10.3204/XFEL.EU/TR-2012-008](https://doi.org/10.3204/XFEL.EU/TR-2012-008).
- [8] T. Tanaka et al., *Nuclear Instruments and Methods in Physics Research Section A: Accelerators, Spectrometers, Detectors and Associated Equipment* **659**, 528–530 (2011)
DOI: [10.1016/j.nima.2011.08.039](https://doi.org/10.1016/j.nima.2011.08.039).
- [9] T. Tanaka et al., *Review of Scientific Instruments* **86**, 093104 (2015)
DOI: [10.1063/1.4929666](https://doi.org/10.1063/1.4929666).
- [10] T. Tanaka et al., *Metrologia* **53**, 98 (2016)
DOI: [10.1088/0026-1394/53/1/98](https://doi.org/10.1088/0026-1394/53/1/98).
- [11] A. Gottwald et al., *Measurement Science and Technology* **21**, 125101 (2010)
DOI: [10.1088/0957-0233/21/12/125101](https://doi.org/10.1088/0957-0233/21/12/125101).
- [12] B. L. Henke et al., *Atomic Data and Nuclear Data Tables* **54**, 181–342 (1993)
DOI: [10.1006/adnd.1993.1013](https://doi.org/10.1006/adnd.1993.1013).
- [13] S. Klumpp et al., *Design of an optimized XGM*, (EUCALL Milestone M7.1, 2016).
- [14] K. Tiedtke et al., *AIP Conference Proceedings* **705**, 588–592 (2004)
DOI: [10.1063/1.1757865](https://doi.org/10.1063/1.1757865).

